The effects of bracket, wire conformation and size on the load systems during orthodontic sliding mechanics

David E. Mika
Private practice
Perry, Michigan

Thomas R. Katona
Associate Professor
Department of Orthodontics and Oral Facial Genetics, Indiana University School of Dentistry
Department of Mechanical Engineering, Purdue University School of Engineering and Technology
IUPUI, Indianapolis, IN

Corresponding author
Dr. Thomas R. Katona
Indiana University School of Dentistry
1121 W. Michigan St., Indianapolis, IN 46202

tkatona@iu.edu

ABSTRACT

Objective: The purpose of this laboratory study was to compare all 6 load components (3 force and 3 moment) acting on 2 different stainless steel brackets as they slide along 3 sizes of stainless steel archwires with 3 different conformations.

Materials and Methods: Brackets were attached to a load cell and elastomeric ligated to the wires. As the load cell was pulled along a precision track, the 6 load components (forces and moments in the 3 orthogonal coordinate system) acting on the bracket were recorded. ANOVA was applied to the data.

Results: Overall, there were significant differences for all effects (bracket, wire size and wire configuration), for all outcomes (the loads), except the effect of bracket on the force of friction and one of the moment components.

Conclusion: The results demonstrate that the force of friction associated with sliding mechanics should not be considered in isolation, because factors that affect it also affect the other 5 load components.

KEY WORDS: Orthodontic brackets; Wires; Ligation; Friction; Forces; Moments

INTRODUCTION

Friction between orthodontic brackets and archwires is a well-researched topic. Many combinations of bracket designs and materials (titanium, stainless steel, ceramic) and wire cross-sections (rectangular, square, round, and braided) of differing sizes and materials (stainless steel, nickel titanium, TMA), with various ligations (elastic, stainless steel, self-ligating) have been studied.[1-6]

Patients' dentitions follow unique curvatures, and wire shape is also site-specific along the arch. Furthermore, wires are likely to be locally distorted due to misaligned teeth. It is therefore expected that the load (force and moment) components (one of which is the force of friction) between wire and bracket would change with position along the arch. (This generally neglected curvature of tooth travel also requires a modified analytical approach.[7]) However, all but two published benchtop studies[8, 9] deal with friction along a straight archwire, and only one of them[9] also considers the other concomitant force/moment components.

The purpose of this study was to determine how the complete load system (the 3 force and 3 moment components), not just the force of friction component, **Figure 1**, between different wires and brackets depend on archwire conformation.

MATERIALS AND METHODS

All 6 load components acting on the bracket were simultaneously measured as 2 bracket sizes were slid along 3 archwire cross-sections in 3 configurations, with movement in 2 directions.

The brackets were mandibular stainless steel 0.022-in slot twin brackets (Victory Series Twin Brackets, 3M Unitek, Monrovia, California). Central incisor and canine brackets were chosen for having a relatively large width difference, 2.5 and 3.2 mm, respectively. Three stainless steel wires (Ormco, Orange, California, 0.018-in round, 0.016 x 0.016-in, and 0.021 x 0.021-in) were tested. (The area moment of inertia (stiffness) of a round wire, with diameter d, is given by $I_{\bullet} = \pi d^4/64$. Similarly, that of a square wire with sides a, $I_{\blacksquare} = a^4/12$. Thus, I = 5.15E-09, 5.46E-09 and 1.62E-08 inch^4 for the 3 wires, respectively, or ratios of 1.00/1.06/3.15 .)

The testing apparatus consisted of a bracket that was attached to a load cell, which, in turn, was pulled along a precision track (**Figure 1**). The orthodontic wire that was ligated into the bracket was held in a fixed, but adjustable, holder (**Figures 2** and **3**).

Specimen Preparation

Each bracket was attached to a hex-drive bolt head (**Figures 1**, **3** and **4**) as follows. The hex hole was drilled-out just large enough, and about 1/8 inch deep, to envelop the bracket base. The hole was filled with orthodontic resin (Dentsply, Milford, DE), and the bracket base was embedded in the uncured composite. The flash was gently folded over the bracket base to increase retention, and then the composite was pre-cured with a Mini LED Ortho light (American Orthodontics, Sheboygan, Wisconsin) for approximately 10 seconds. If present, excess composite was gently removed with a hand scaler.

To position the bracket prior to the final cure, an alignment jig (**Figure 4**) was used. The jig consisted of two lower canine "brackets-in-bolt" like the specimens described in the previous paragraph. (The brackets were positioned so that no torque would be expressed.) They were screwed into threaded holes in a steel plate, their slots were aligned, and tightened. Then, for the final cure of the specimen, it was threaded into a hole midway between the other screws, a straight section of 0.021 x 0.025-in stainless steel wire was ligated onto the three brackets with elastomeric ligatures (3M Unitek AlastiK Easy-to-Tie Ligatures Size A-1, 0.125 in Outer Diameter), and the specimen was final cured for 10 seconds. Finally, flash, if any, was gently removed to fully expose the wings.

Apparatus

The Gamma load cell/bracket assembly (ATI Industrial Automation, Apex, NC) was mounted on a precision track (Mini-Guide, Double Carriage, Model #SEBS 9BUU2-195, Nippon Bearing Co, Japan; **Figures 1** and **3**). The load cell measures all 3 force (0-65 ± 0.2 N) and all 3 moment (0-5 ±0.0009 N-m) components. Weights, lowered and raised by an MTS Bionix 858 (MTS Corp., Minneapolis, MN) mechanical testing machine, pulled the load cell along the track with an arrangement (**Figures 1** and **3**) that was intended to protect the load cell from overload. The wire mount (**Figures 2** and **3**) was stationary, but adjustable relative to the track, **Figure 2**. The mount was an aluminum plate with a 2" long x 1" wide window in the middle. The load cell moved parallel to the 1" side. The mount included guides to maintain parallelism during set-up adjustments, **Figures 2** and **3**.

For each wire size, a pair of (1 x 4 x ¼ inch) aluminum clamps was fabricated, **Figure 2**. Each had a slot wide enough to accommodate the wire, yet sufficiently shallow to leave the wire slightly exposed. When C-clamped to the aluminum mounting plate at the 2 sides of its opening, the ends of the wire were rigidly attached. One plate was kept in place, while the other was positioned with shims to obtain the wire shapes, **Figure 2**.

Testing set-up

The bolt/bracket specimen was placed into a slightly tightened rigid shaft coupling (generic) on the load cell. A wire was aligned in the mount in the initial 0° (aligned) orientation and clamped to the mounting plate with the custom clamps (**Figures 2** and **3**). The plate was moved around so that the wire could be passively engaged into the bracket when it was raised into contact, with the bolt ~ ½ mm from the edge of the opening, **Figure 2A**. The mounting plate was tightened and the bracket was held in position with an elastomeric ligature. The rigid shaft coupling was fully tightened to secure the specimen to the load cell.

Testing procedure

The MTS machine was programmed to raise and lower the 10# weight (counterweighted with 5#) a distance of 5 mm, in a 0.2 Hz ramp mode, **Figure 1C**. This translated in the load cell/bracket specimen assembly moving back-and-forth 5 mm along the wire (**Figure 2A**) while the load cell's 6 load component readings were recorded at a rate of 10/second. In general, 5 - 6 round trips were completed, but only the last 3 full cycles were analyzed. Then, a series of 5 ligatures were placed to generate 5 sets of data.

The right wire clamp was shimmed 0.018 inch to produce an effective (θ =) 1° curved misalignment between wire and bracket path, **Figures 2C** and **2D**. Data were obtained, as above. Then, an effective (θ =) 2° misalignment curve was created with a 0.035 inch shim. The complete set of tests described above was then repeated with the 2 other wires. Isopropyl alcohol wire cleaning, load cell zeroing, and wire/bracket aligning were performed during wire changes.

Then, the entire test was repeated with the 2nd bracket.

Data Sets and Data Acquisition

There was a total of 18 (2 brackets x 3 wires x 3 arch shapes) kinds of specimens. With each one, the bracket was slid 5 mm forward, then 5 mm in reverse, back to the starting point. The 6 load components were measured continuously during the roundtrips and analyzed separately. Five elastomeric ligatures were used, for about 5 round trips each, to obtain data for 18 total runs.

The incisor bracket was tested first with all wires at the 0° deformation. Then, we tested the stiffest archwire (0.021 x 0.021-in) with 2° deformation and determined that a larger angle could overload the load cell. Thus, the use of 0°, 1° and 2°. The 0° - 2° - 1° sequence was used with the remaining archwires. Then, the tests were repeated with the canine bracket.

Statistical Methods

Summary statistics (mean, standard deviation, standard error, minimum, maximum) for the 6 load components were calculated for each of the bracket-archwire-arc shape combinations in the forward and reverse displacement directions. The effects of bracket, archwire, arc shape, and displacement direction on the load components were analyzed using ANOVA, which included fixed effects for each of the four factors and their interactions and a random effect to allow correlation between the measurements from forward and reverse displacement on each wire. Pair-wise comparisons were performed using Fisher's Protected Least Significant Differences to control the overall significance level at 5%. Distributions of the measurements were examined, and a transformation of the data was used to satisfy the ANOVA normal distribution assumption. The homogeneous variance assumption was also evaluated, and heterogeneous variances were allowed.

A log transformation (of absolute values) of the data was performed prior to the analyses. The means of outcomes Fx, Fy, Fz, Mx, My, and Mz were calculated for the three right and three left cycles, for each of the 5 repeated bracket-wire-angle sets, and these values were used for the analyses. The model included main effects for bracket, wire, and angle, and a random effect for the direction (left/right), for the outcomes Fx, Fy, Fz, Mx, My and Mz.

RESULTS

Examples of collected data are presented for 4 out of the 18 configurations in **Figure 5**. Overall, there were significant differences for all effects, for all outcomes, except the effect of bracket for outcomes Fx (friction) and My.

<u>Fx (force of friction)</u>

For Fx, the incisor bracket was not significantly different than the canine bracket (P = .8710). The 0.016 x 0.016-in wire was significantly lower than the 0.021 x 0.021-in and 0.018-in wires ($P < .0001$), and the 0.018-in wire was significantly lower than the 0.021 x 0.021-in wire ($P < .0001$). 0° was significantly lower than the 1° and 2° ($P < .0001$) offsets, and the 1° was significantly lower than the 2° ($P = .0032$).

<u>Fy</u>

For Fy, the canine bracket was significantly lower than the incisor bracket ($P < .0001$). The 0.016 x 0.016-in wire and the 0.018-in wire were significantly lower than the 0.021 x 0.021-in wire ($P < .0001$), but the 0.016 x 0.016-in wire and 0.018-in wire were not significantly different (*P* = .2781). The 0° shape was significantly lower than the 1° and 2° (*P* < .0001), and 1° was significantly lower than 2° (*P* < .0001).

<u>Fz</u>

For Fz, the canine bracket was significantly lower than the incisor bracket (*P* < .0001). The 0.016 x 0.016-in wire was significantly lower than the 0.021 x 0.021-in and 0.018-in wires (*P* < .0001), and the 0.018-in wire was significantly lower than the 0.021 x 0.021-in wire (*P* = .0117). The 0° shape was significantly lower than the 1° and 2° (*P* < .0001), but 1° was not significantly different than 2° (*P* = .3747).

<u>Mx</u>

For Mx, the canine bracket was significantly lower than the incisor bracket (*P* < .0001). The 0.016 x 0.016-in wire was significantly lower than the 0.021 x 0.021-in wire (*P* < .0001), and the 0.018-in wire was significantly lower than the 0.021 x 0.021-in wire (*P* < .0001). The 0.016 x 0.016-in wire was not significantly different than the 0.018-in wire (*P* = .1080). 0° was significantly lower than 1° and 2° (*P* < .0001), and 1° was significantly lower than angle 2° (*P* < .0001).

<u>My</u>

For My, the brackets were not significantly different (*P* = .2534). The 0.016 x 0.016-in wire was significantly lower than the 0.021 x 0.021-in and the 0.018-in wires (*P* < .0001), and the 0.018-in wire was significantly lower than the 0.021 x 0.021-in wire (*P* < .0001). The 0° shape was significantly lower than 1° and 2° (*P* < .0001), and 1° was significantly lower than 2° (*P* = .0033).

<u>Mz</u>

For Mz, the incisor bracket was significantly lower than the canine bracket (*P* < .0001). The 0.016 x 0.016-in wire was significantly lower than the 0.018-in wire (*P* = .0022) and the 0.021 x 0.021-in wire (*P* < .0001), and the 0.018-in wire was significantly lower than the 0.021 x 0.021-in wire (*P* < .0001). 0° was significantly lower than 1° and 2° (*P* < .0001), and 1° was significantly lower than 2° (*P* = .0007).

In all tests, except for Fz in some tests, all 6 load components increased with increasing wire offset. Differences in loads associated with bracket size were inconsistent. The canine bracket was significantly lower in Fy, Fz, and Mx, while the narrower incisor bracket was significantly lower in Mz. There was no difference in Fx or My.

Except for Fy and Mx, the 0.016 x 0.016-in wire was significantly lower than the 0.018-in and 0.021 x 0.021-in wires. Also, the 0.018-in wire was significantly lower than the 0.021 x 0.021-in wire. For Fy and Mx, the only difference was that the two smaller wires, 0.016 x 0.016-in and 0.018-in, were not significantly different from one another, though both were significantly lower than the 0.021 x 0.021-in wire.

DISCUSSION

This experiment was designed to examine phenomena involved in sliding mechanics. Thus, perceived limitations may be attributed to the lesser priority given to clinical simulation.

For example, we did not test a 0.019 x 0.025-in wire which is typically used with the 0.022-in slot, but the tested 0.021 x 0.021-in wire is seldom, if ever, used in sliding mechanics. However, for our purposes, it was far more important to have wire cross sections with the relative stiffness spread described above. These, and other potential concerns, such as the effects of saliva (lubrication), could be addressed in future studies.

Due to their relatively large moment arms, Fx and Fy are the major contributors to My and Mx, respectively. Therefore, it is somewhat expected that Fx and My, and Fy and Mx, would mirror behaviors. Differences, if any, in the results for the 0.018 and the 0.016 x 0.016 wires vs. the results for the 0.021 x 0.021 wire could be explained by wire stiffness since the two thinner wires' area moments of inertia are similar, but about 1/3 that of the thicker 0.021 x 0.021 wire. The snugness of bracket-slot fit would be another possible explanation. The similarity of results for the 2 thin wires could be attributable to similar stiffnesses, while differences could be ascribed to their different fits (round vs. square) into the slots.

Thus, overall, except for Fx (friction) and My being unaffected by bracket, all changes in bracket and wire size and configuration caused significant differences in all loads (Fx, Fy, Fz, Mx, My, Mz) on the bracket. In a very limited sense, these results are similar to previously published[8] data in that the increase in wire curvature caused an increase in friction force, Fx. But in addition, the results of this study clearly demonstrate that parameters that affect the force of friction can also have profound effects on the other 5 load components. A similar conclusion was reached in the previous study,[9] but their focus was on archwire composition.

It is known that sliding occurs in fits-and-starts during clinical tooth movement. Although the biological support system (tooth - PDL - bone) is clearly different from the experimental structure (bolt - load cell - track), the same behavior can be seen in the ragged friction (Fx) force component shown in **Figure 5**, particularly at the higher values, **Figure 5D**.

CONCLUSION

The results of this study demonstrate that the force of friction (Fx) associated with sliding mechanics should not be considered in isolation. In general, factors that affect it also affect the other 5 load components.

REFERENCES

1. Articolo LC, Kusy RP. Influence of angulation on the resistance to sliding in fixed appliances. *Am J Orthod Dentofacial Orthop.* 1999;115:39-51.
2. Thorstenson GA, Kusy RP. Effects of ligation type and method on the resistance to sliding of novel orthodontic brackets with second-order angulation in the dry and wet states. *Angle Orthod.* 2003;73:418-430.
3. Hain M, Dhopatkar A, Rock P. The effect of ligation method on friction in sliding mechanics. *Am J Orthod Dentofacial Orthop.* 2003;123:416-422.
4. Hain M, Dhopatkar A, Rock P. A comparison of different ligation methods on friction. *Am J Orthod Dentofacial Orthop.* 2006;130:666-670.
5. Kumar S, Singh S, Hamsa PRR, Ahmed S, Prasanthma, Bhatnagar A, et al. Evaluation of friction in orthodontics using various brackets and archwire combinations-an in vitro study. *J Clin Diagn Res.* 2014;8:ZC33-36.

6. Vinay K, Venkatesh MJ, Nayak RS, Pasha A, Rajesh M, Kumar P. A comparative study to evaluate the effects of ligation methods on friction in sliding mechanics using 0.022" slot brackets in dry state: An In-vitro study. *J Int Oral Health.* 2014;6:76-83.
7. Katona TR, Isikbay SC, Chen J. An analytical approach to 3D orthodontic load systems. *Angle Orthod.* 2014;84:830-838.
8. Fourie Z, Ozcan M, Sandham A. Effect of dental arch convexity and type of archwire on frictional forces. *Am J Orthod Dentofacial Orthop.* 2009;136:14 e11-17; discussion 14-15.
9. Kroczek C, Kula K, Stewart K, Baldwin J, Fu T, Chen J. Comparison of the orthodontic load systems created with elastomeric power chain to close extraction spaces on different rectangular archwires. *Am J Orthod Dentofacial Orthop.* 2012;141:262-268.

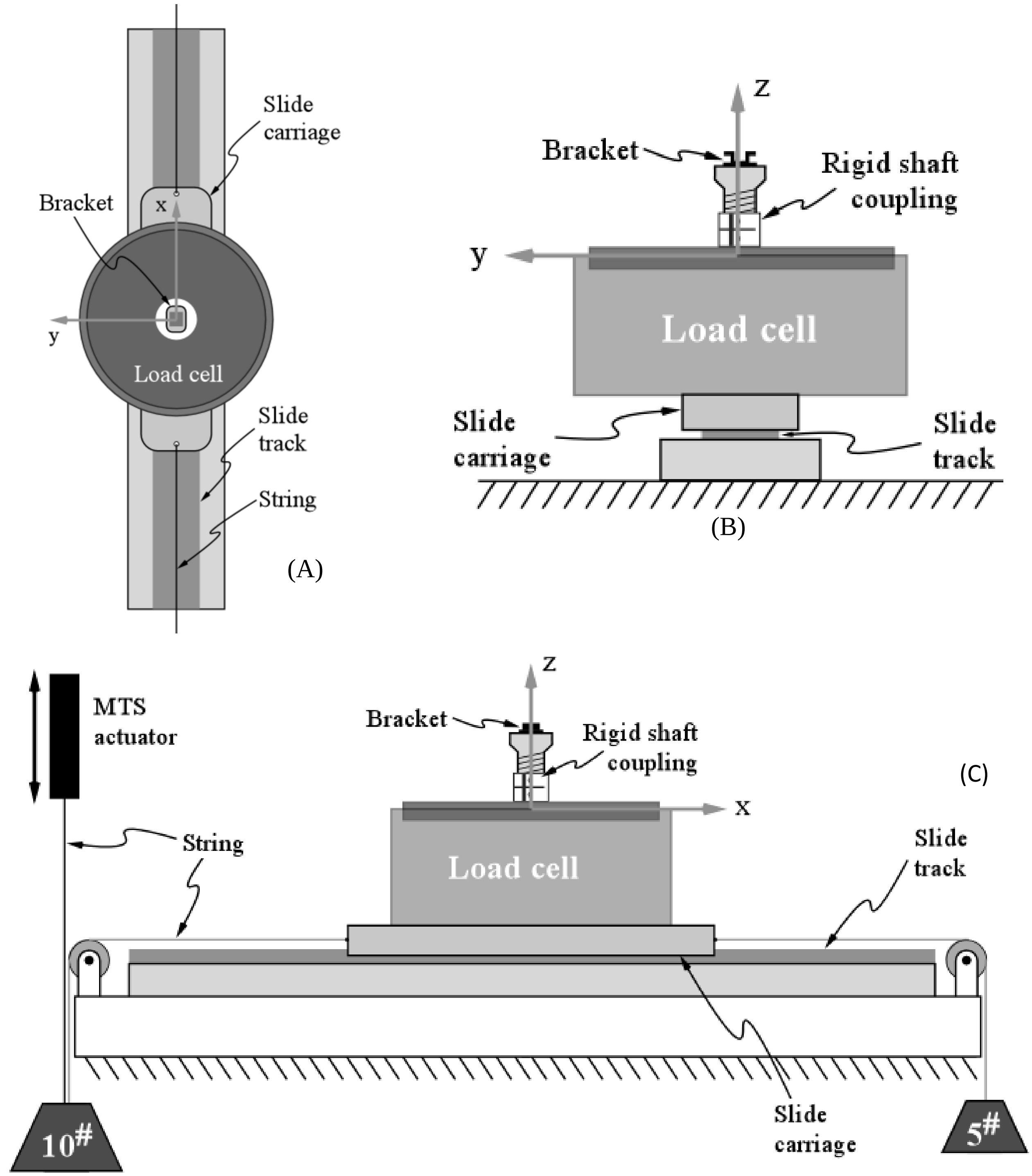

Figure 1. (A) Schematic of the top view of slide – load cell – bracket assembly. (B) Back view. (C) Side view. In the position shown, if the actuator lifts the 10# weight, the 5# weight pulls the load cell to the right. If the actuator lowers the 10#, then the 10# weight pulls the load cell to the left.

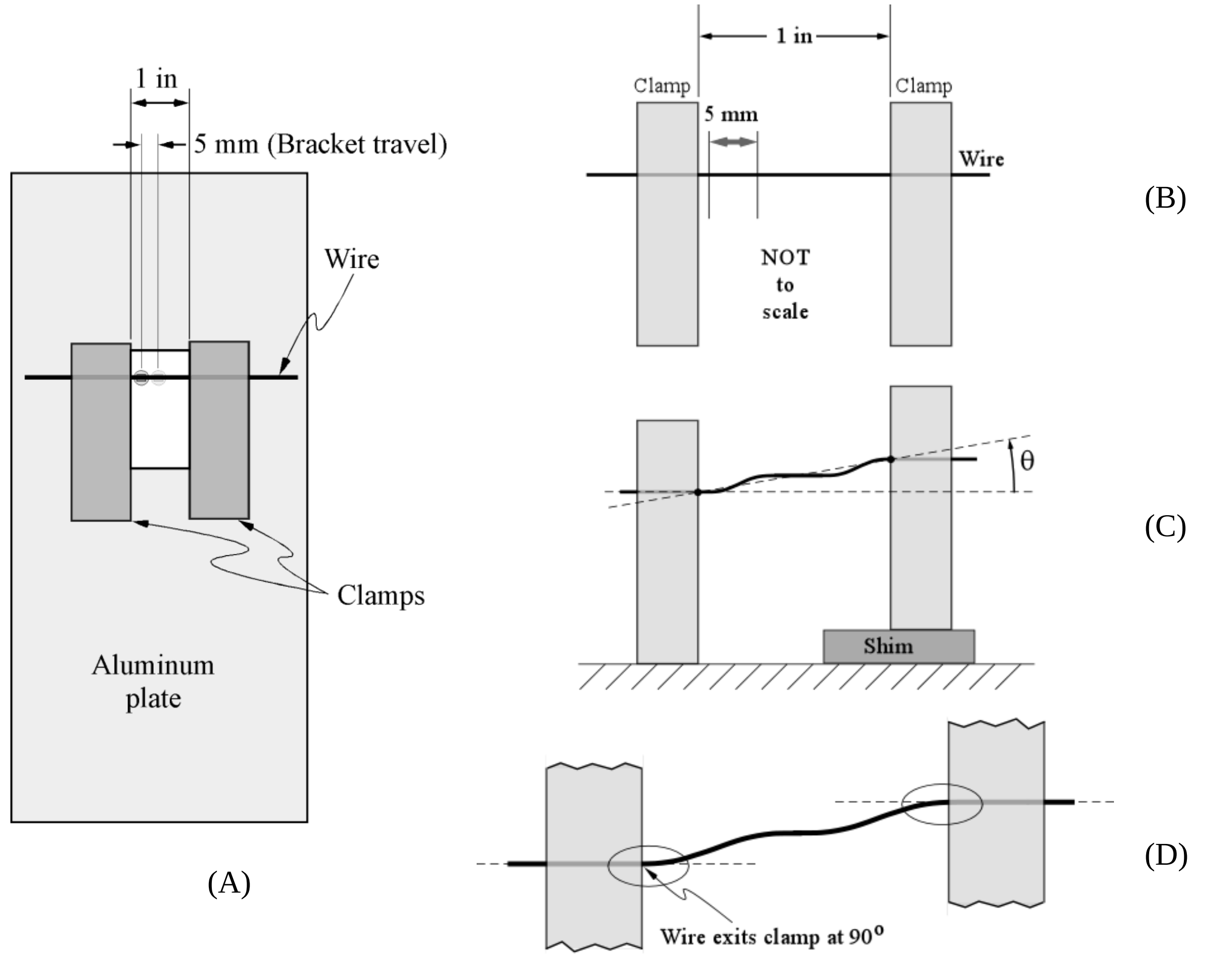

Figure 2. (A) Schematic of wire holder. (B - D) Wire holder clamps control wire configuration. A cantilevered (fixed) wire emerges from the supports in a straight line, at 90° to the clamp in this design, which mimics a bracket or tube. When the supports are kept parallel, but shifted relative to each other, an "S" shape conformation is imposed on the wire. The offset angle, θ, is used to characterize the deformed wire.

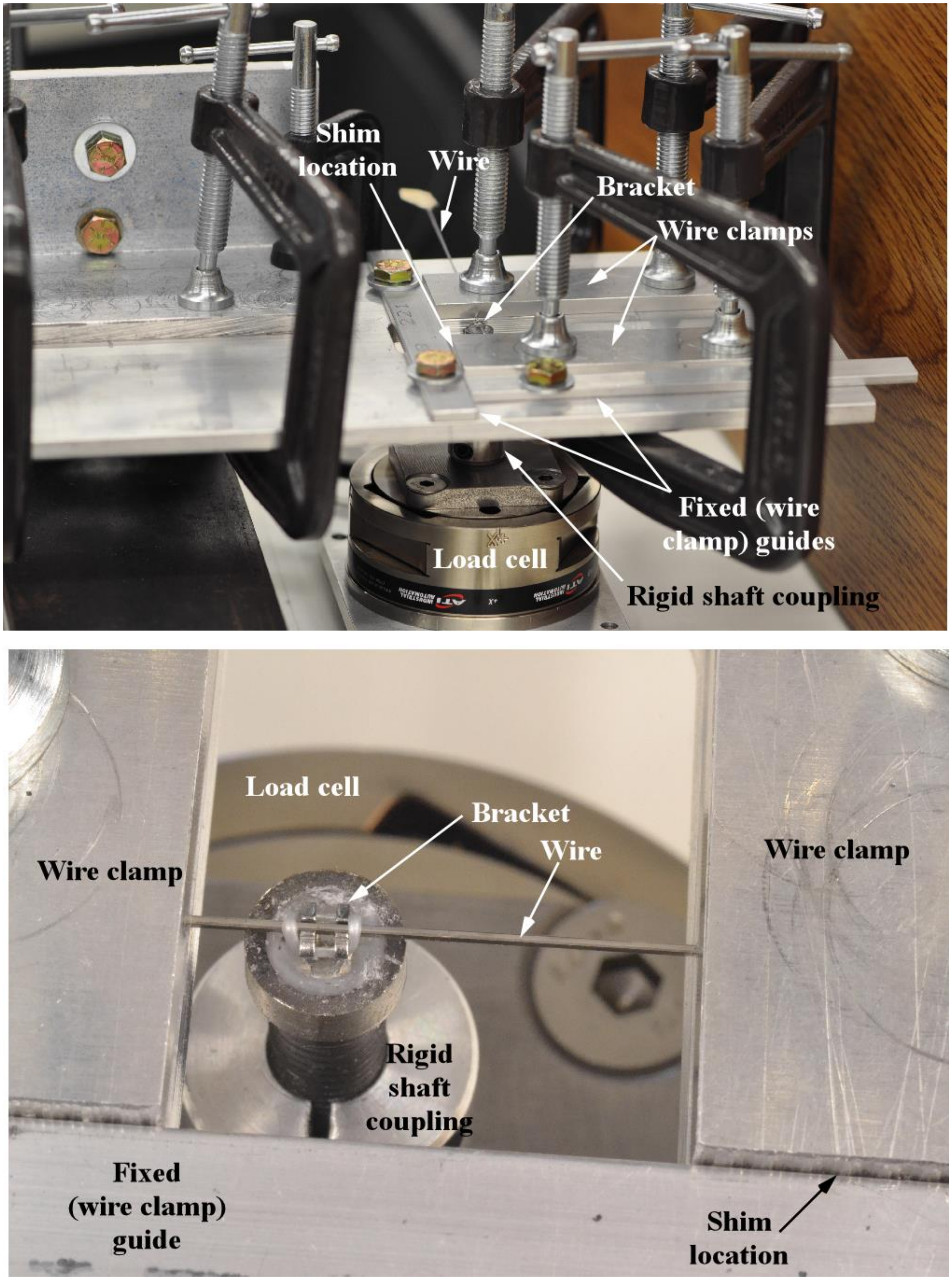

(A)

(B)

Figure 3. (A) Assembled apparatus. (B) Bracket assembly while moving to the right. (Note “dragging” ligature on left side.)

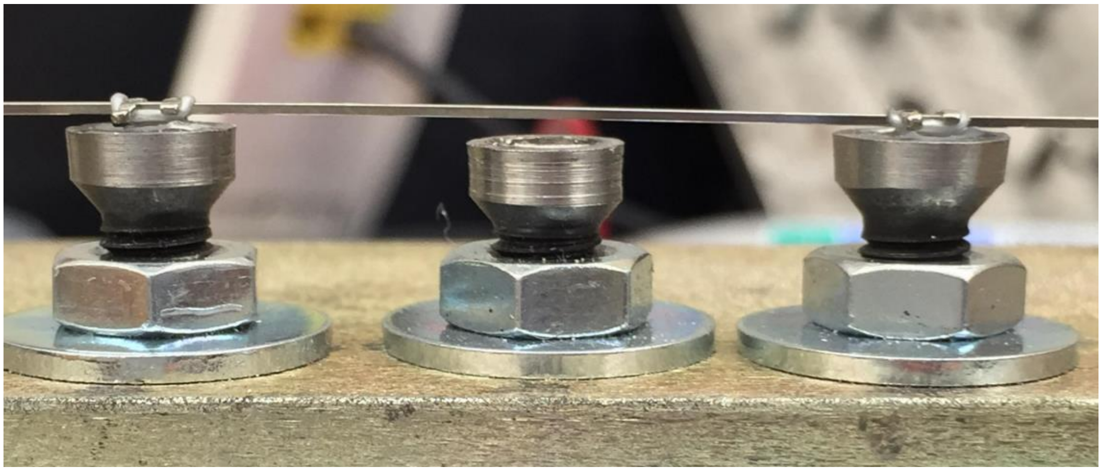

Figure 4. Mounting jig. Two canine bracket/bolt assemblies were used as "abutments" to align specimen bracket (not shown) with ligated wire during its cure inside the drilled-out bolt head (center).

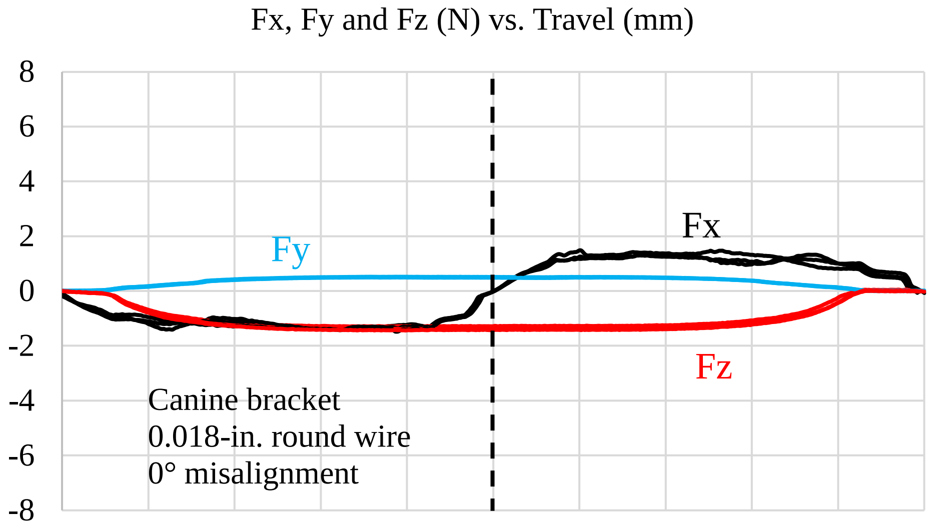
Fx, Fy and Fz (N) vs. Travel (mm)
8
6
4
2
0
-2
-4
-6
-8
Fy
Fx
Fz
Canine bracket
0.018-in. round wire
0° misalignment

(5A)

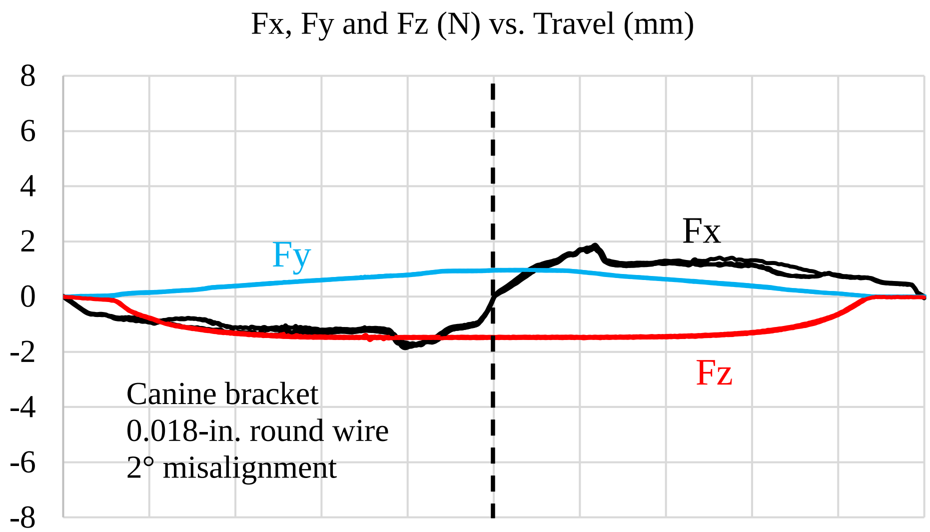
Fx, Fy and Fz (N) vs. Travel (mm)
8
6
4
2
0
-2
-4
-6
-8
Fy
Fx
Fz
Canine bracket
0.018-in. round wire
2° misalignment

(5B)

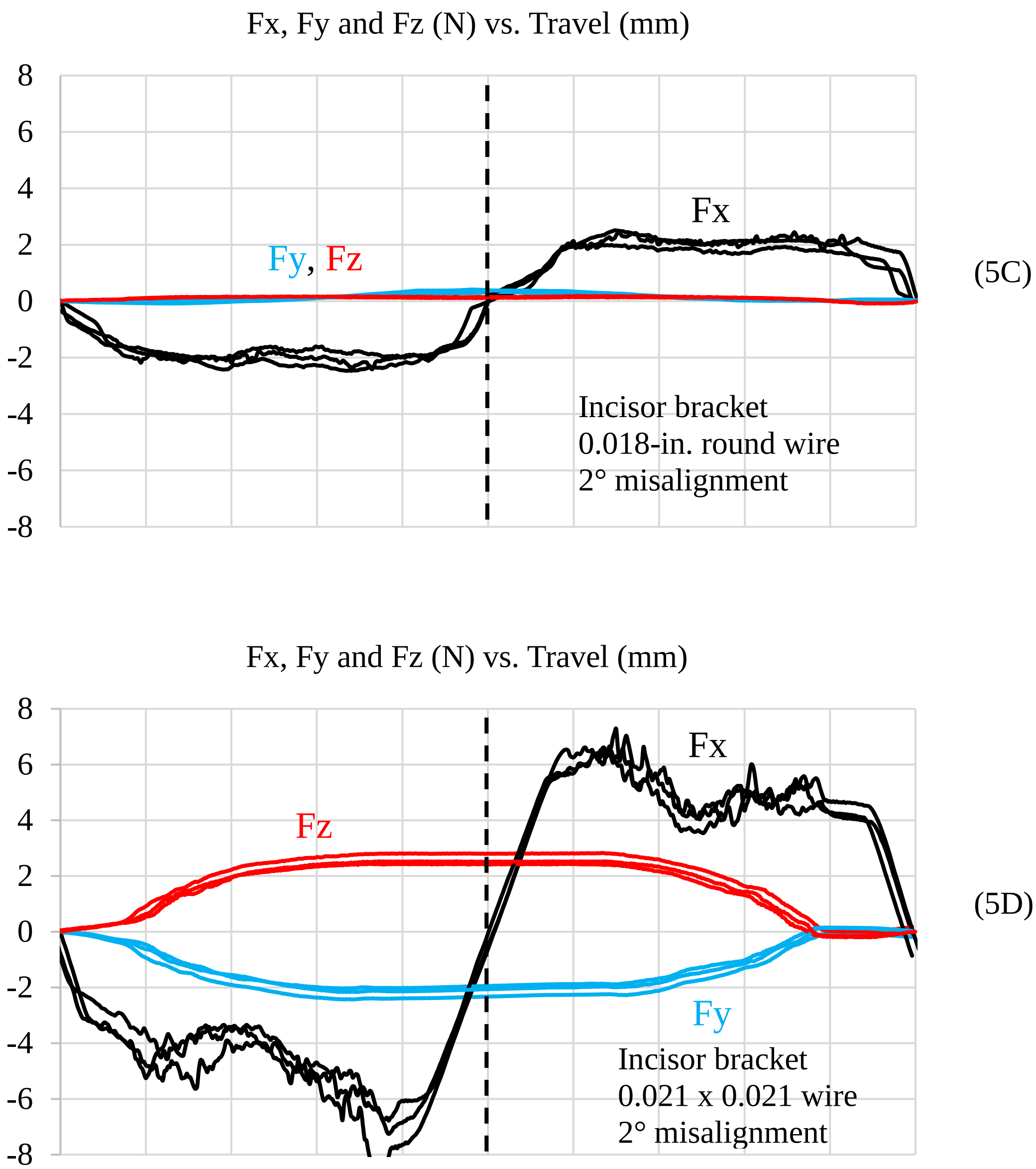

Figure 5. Examples of selected results for Fx (friction), Fy and Fz. Vertical dashed lines demarcate direction change during 1 complete cycle. Distance between vertical lines can be interpreted as 250 data points, 5 mm of bracket travel or 2.5 seconds. 3 complete cycles are shown.